VIRGIL C. SUMMER NUCLEAR STATION (VCSNS)
DOCKET NO. 50-395
OPERATING LICENSE NO. NPF-12

Attachment 3

LTR-PAFM-12-137-NP, Revision 1

LTR-PAFM-12-137-NP

Revision 1

Technical Basis for Westinghouse Embedded Flaw Repair for V. C. Summer Unit 1 Reactor Vessel Head Penetration Nozzles

November 2012

Author: C. K. Ng*
Piping Analysis and Fracture Mechanics

Verifier: A. Udyawar*
Piping Analysis and Fracture Mechanics

Approved: S. A. Swamy*
Manager, Piping Analysis and Fracture Mechanics

*Electronically approved records are authenticated in the Electronic Document Management System

Westinghouse

Record of Revisions

Revision	Date	Description of Changes
0	October 2012	Original Issue
1	November 2012	Incorporate NRC comments and information from the latest NDE data sheet

Note :

Changes made in the latest revision are indicated by a single line in the right hand margin as shown here.

1 INTRODUCTION

As a part of the inspection and contingence repair efforts associated with the reactor vessel closure head inspection program at V. C. Summer Unit 1, engineering evaluations were performed to support plant specific use of the Westinghouse embedded flaw repair process to repair unacceptable flaws detected in the head penetration nozzles during the Fall 2012 outage. The embedded flaw repair process involves depositing a weld material, which is Primary Water Stress Corrosion Cracking (PWSCC) resistant, over the detected flaw on the outside surface of the penetration nozzle of interest as well as over the wetted surface of the attachment J-groove weld. As a result, the surface flaw becomes a sub-surface flaw and is no longer exposed to the primary water environment. The methodology used is based on extensive analytical work completed by the Westinghouse Owners Group, currently the Pressurized Water Reactor Owners Group (PWROG), and a large collection of test data obtained under the sponsorship of Westinghouse, Babcock & Wilcox (B&W) and the former Combustion Engineering Owners groups (CEOG), as well as the Electric Power Research Institute (EPRI). The technical basis of the embedded flaw repair process is documented in WCAP-15987-P Revision 2-P-A [1] and has been reviewed and accepted by the Nuclear Regulatory Commission (NRC) in the United States. In the NRC Safety Evaluation Report that was incorporated in WCAP-15987-P Revision 2-P-A, the NRC staff concluded that, subject to the specified conditions and limitations, the embedded flaw repair process described in WCAP-15987-P provides an acceptable level of quality and safety. The staff also concluded that WCAP-15987-P is acceptable for referencing in licensing applications.

In this report, the technical basis and the flaw evaluation results to support the use of the Westinghouse embedded flaw repair process for head penetration nozzle number 19, 31, 37 and 52 with unacceptable outside surface flaws in the vicinity of the J-groove weld toes are provided. Engineering evaluations were performed to determine the maximum acceptable initial flaw sizes that can be left behind in a repaired penetration nozzle which would satisfy the ASME Section XI requirements [2]. The purpose of this report is to provide plant-specific technical basis for the use of the embedded flaw repair process and to confirm that V. C. Summer Unit 1 meets the criteria for application of the embedded flaw repair process stated in Appendix C of WCAP-15987-P [1].

2 TECHNICAL BASIS FOR APPLICATION OF EMBEDDED FLAW REPAIR PROCESS TO HEAD PENETRATION NOZZLES

This section provides a discussion on the technical basis for the use of embedded flaw repair process for head penetration nozzle number 19, 31, 37 and 52 with unacceptable outside surface flaws. Such a repair involves depositing several layers of Alloy 52/52M weld material over the flaw on the outside surface of the penetration nozzle of interest below the J-groove weld as well as the wetted surface of the attachment J-groove weld. Since the Alloy 52/52M repair weld material is PWSCC resistant, the detected surface flaw in the head penetration nozzle of interest is then shielded from the primary water environment and is no longer susceptible to primary water stress corrosion cracking.

For the repair of the unacceptable outside surface flaws in head penetration nozzle number 19, 31, 37 and 52, at least three layers of Alloy 52/52M material are deposited (360° full circumference) covering the entire wetted surface of the attachment J-groove weld. The repair weld extends at least 0.5 inch past the interface between the J-groove weld buttering and stainless steel cladding as well as covering the entire outside surface of the head penetration nozzle with at least two layers of Alloy 52/52M material. A schematic of the repair configuration for the repaired outside surface flaw is illustrated in Figure 2-1.

Flaw evaluations were performed based on the flaw sizes and shapes remaining in the repaired head penetration nozzles of interest to demonstrate that the left behind flaws are acceptable for continued operation. The as-found flaw parameters for penetration nozzle number 19, 31, 37 and 52 are shown below in Table 2-1. Since all the indications located on the outside surface of the penetration nozzles in the vicinity of the attachment J-groove weld toes are skewed with respect to the axis of the penetration nozzles, both axial and circumferential flaws are assumed.

Table 2-1
As-Found Flaw Parameters in V. C. Summer Unit 1 Head Penetration Nozzles

Indications	Flaw Orientation	Flaw Length (in)	Flaw Depth (in)	Flaw Location
Penetration No. 19 (Indications #1 & #2)	Circumferential	1.36	0.283	Outside Surface/Downhill Side
	Axial	0.72		
Penetration No. 31 (Indication #1)	Circumferential	0.16	0.122	Outside Surface/Downhill Side
	Axial	0.52		
Penetration No. 31 (Indication #2)	Circumferential	0.16	0.177	Outside Surface/Downhill Side
	Axial	0.36		
Penetration No. 31 (Indication #3)	Circumferential	0.26	0.256	Outside Surface/Downhill Side
	Axial	0.61		
Penetration No. 37 (Indication #1)	Circumferential	0.31	0.249	Outside Surface/Downhill Side
	Axial	0.76		
Penetration No. 37 (Indication #2)	Circumferential	0.10	0.214	Outside Surface/Downhill Side
	Axial	0.56		
Penetration No. 37 (Indication #3)	Circumferential	0.16	0.294	Outside Surface/Downhill Side
	Axial	0.52		
Penetration No. 52 (Indication #2)	Circumferential	0.47	0.279	Outside Surface/Downhill Side
	Axial	0.32		
Penetration No. 52 (Indication #3)	Circumferential	0.21	0.132	Outside Surface/Downhill Side
	Axial	0.12		

Based on the Ultrasonic Testing (UT) and Penetrant Testing (PT) results at the regions of interest for penetration nozzle number 19, 31, 37 and 52, there are no surface connected indications in the J-groove weld and the detected indications are solely in the base metal of the nozzles. Each of the detected UT indications starts in the nozzle below the toe of the weld. Some of the measured indication lengths extend slightly above the toe of the weld, but the measurement technique overestimates the lengths due to the large beam spread inherent with tip diffraction probes. The thinnest portion of the weld is the ground contour that blends the weld to the nozzle, so any propagation from the nozzle base metal into the weld metal would be expected to start at that point. In order to determine if the indications grew into the weld metal at this contoured section of the weld, a PT was performed on the J-groove weld and adjacent nozzle. Since none of the PT indications continued into the J-groove weld, it was concluded that the indications only involve the base metal of the nozzle. The technical basis for the embedded flaw repair provided is therefore focused on the indications in the base metal of the penetration nozzles of interest.

2.1 EVALUATION PROCEDURE AND ACCEPTANCE CRITERIA

Rapid, non-ductile failure is possible for ferritic materials at low temperatures, but is not applicable to the nickel-base alloy head penetration nozzle material such as Alloy 600. Nickel-base alloy material is a high toughness material and plastic collapse would be the dominant mode of failure. Therefore the evaluation procedures and acceptance criteria for indications in austenitic piping contained in paragraph IWB-3640 of ASME Section XI Code [2] are applicable for evaluation of flaws in the head penetration nozzles. The evaluation procedure used is consistent with those in Appendix C of WCAP-15987-P [1] and summarized below:

2.1.1 Acceptance Criteria for Axial Flaws

For axial flaws, the allowable flaw depth for a given flaw length can be determined from the following expression:

$$\sigma_h = \frac{\sigma_f}{SF_m}\left[\frac{1-\frac{a}{t}}{1-\left(\frac{a}{t}\right)\Big/ M_2}\right]$$

where

$$M_2 = \left[1+\left(\frac{1.61}{4R_m t}\right)\ell^2\right]^{1/2}$$

and

σ_f = Flow stress = $\frac{S_u + S_y}{2}$ (Average of Ultimate and Yield Strengths)
σ_h = PR_m/t
ℓ = Total Flaw Length
a = Flaw Depth
R_m = Mean Radius of Penetration Nozzle
t = Wall Thickness of Penetration Nozzle
P = Internal Pressure
SF_m = Safety Factor for membrane stress:
2.7 for Level A Service Loading
2.4 for Level B Service Loading
1.8 for Level C Service Loading
1.3 for Level D Service Loading

The limits of applicability of this equation are $a/t \leq 0.75$ and $\ell < \ell_{allow}$, where

$$\ell_{allow} = 1.58(R_m t)^{0.5}[(\sigma_f/\sigma_h)^2 - 1]^{0.5}$$

This limit is chosen such that surface flaws would remain below the critical size based on the plastic collapse condition if they should grow through the wall.

2.1.1 Acceptance Criteria for Circumferential Flaws

For circumferential flaws, the following relationship between the applied loads and flaw depth at incipient collapse given by equations in ASME Section XI Article C-5000 [2] is used:

$$\sigma_b^c = \frac{2\sigma_f}{\pi}\left[2\sin\beta - \frac{a}{t}\sin\theta\right]$$

$$\beta = \frac{1}{2}\left(\pi - \frac{a}{t}\theta - \pi\frac{\sigma_m}{\sigma_f}\right)$$

where:

σ_b^c = Bending stress at incipient plastic collapse
θ = One-half of the final flaw angle
β = Angle to neutral axis of penetration nozzle
a/t = Flaw depth to wall thickness ratio
σ_f = Flow stress = $\frac{S_u + S_y}{2}$ (Average of Ultimate and Yield Strengths)
σ_m = Applied membrane stress

The allowable bending stress, S_c, is as follows, which is used to calculate the maximum allowable end-of-evaluation period flaw sizes and the limit of applicability of this equation is $a/t \leq 0.75$.

$$S_c = \frac{\sigma_b^c}{SF_b} - \sigma_m\left[1 - \frac{1}{SF_m}\right]$$

where

S_c = Allowable bending stress for penetration nozzle
σ_m = Applied membrane stress
SF_m = Safety factor for membrane stress
= 2.7, 2.4, 1.8 and 1.3 for Service Level A, B, C, and D respectively
SF_b = Safety factor for bending stress
= 2.3, 2.0, 1.6, and 1.4 for Service Level A, B, C, and D respectively

2.2 Methodology

The flaw evaluation considered that the embedded flaw repair process is used to seal the unacceptable flaws from further exposure to the primary water environment. The evaluation began with the determination of the maximum allowable end-of-evaluation period flaw sizes based on the acceptance criteria described in Section 2.1 for the repaired penetration nozzles. With the embedded flaw repair process, the only mechanism for future sub-critical crack growth is fatigue. The maximum initial embedded flaw size that can remain in a repaired penetration nozzle using the embedded flaw repair process can then be determined by subtracting the predicted fatigue crack growth for future plant operation from the maximum allowable end-of-evaluation period flaw size. This maximum initial allowable embedded flaw size is then compared with the left-behind flaw in the repaired head penetration nozzle of interest to demonstrate acceptability. The following provides a discussion of the loading conditions, geometry, thermal transient stress and fatigue crack growth analysis used in the development of the plant specific technical basis for the embedded flaw repair process.

2.2.1 Geometry and Source of Data

There are many penetration nozzles in the reactor vessel upper head. The outermost penetration nozzles (46.0° intersection angle) were selected for thermal transient and residual stress analysis because the stresses in the outermost penetration nozzles are more limiting and can be used to conservatively represent those at penetration nozzle number 19, 31 and 37 and 52.

The dimensions of all the V. C. Summer Unit 1 penetration nozzles are identical, with a 4.00 inch nominal outside diameter and a nominal wall thickness of 0.625 inch [3]. The distributions of residual, thermal transient and pressure stresses in the upper head penetration nozzle were obtained from the detailed three-dimensional plant specific elastic-plastic finite element analyses [4]. The through-wall stress distributions from the finite element analyses were used

to determine the fatigue crack growth. The resulting crack growth is then used to determine the maximum allowable initial flaw sizes for the left-behind flaws in the repaired penetration nozzles of interest.

2.2.2 Maximum Allowable End-of-Evaluation Period Flaw Size Determination

The requirement for evaluating a flaw using the rules of ASME Section XI is that the loading for normal/upset conditions as well as emergency/faulted conditions be considered. This is necessary because, as discussed in Section 2.1, different safety margins are used for the normal/upset and emergency/faulted conditions. A lower safety factor is used to reflect a lower probability of occurrence for the emergency/faulted conditions.

Plastic collapse is the governing mode of failure for the head penetration nozzles because the high fracture toughness of the nickel base alloy (Alloy 600) material would prevent brittle fracture from occurring. Therefore, it is not necessary to consider the effects of secondary stresses resulting from thermal transient stresses and residual stresses. The governing loading for determining the maximum allowable end-of-evaluation period flaw sizes is therefore those due to internal pressure and other applicable external mechanical loads for the normal, upset, emergency and faulted conditions.

2.2.3 Thermal Transients Used in Fatigue Crack Growth Analysis

For the fatigue crack growth prediction, the effects of secondary stresses resulting from thermal transient and residual stresses must also be considered. The thermal transients that occur in the upper reactor vessel head region are relatively mild. The normal and upset thermal transients considered in the fatigue crack growth calculation are shown in Table 2-2 [5].

Table 2-2
Reactor Coolant System Transients for V. C. Summer Unit 1

Design Transients	Design Cycles
Normal Conditions	
Heat Up/Cooldown	200
Plant Loading/Unloading	18300
Step Load Increase/Decrease	2000
Large Step Load Decrease with Steam Dump	200
Turbine Roll Test	80
Feedwater Heaters Out of Service	40
Steady State Fluctuation (Initial)	150000
Steady State Fluctuation (Random)	3000000
Upset Conditions	
Loss of Load	200
Loss of Flow	80
Loss of Power	40
Reactor Trip From Full Power	400
Inadvertent Auxiliary Spray	10
Excessive Feedwater Flow	30
Operating Basis Earthquake	400

2.2.4 Crack Tip Stress Intensity Factor

One of the key elements in a crack growth analysis is the crack driving force or crack tip stress intensity factor, K_I. This is based on the equations available in the public literature. It should be noted that the flaws in the repaired penetration nozzles are conservatively assumed to be surface flaws even though the flaws are embedded after the repair.

For a part-through wall surface flaw, the stress profile is approximated by a fourth order polynomial as follows:

$$\sigma(x) = A_0 + A_1x + A_2x^2 + A_3x^3 + A_4x^4$$

where:

x = Distance into the wall from the free surface
σ = Stress perpendicular to the plane of the crack
A_i = Coefficients of the 4th order polynomial fit, i = 0, 1, 2, 3, 4

For a surface flaw in the penetration nozzle, the stress intensity factor expression from API-579 [6] is used. The stress intensity factor K_I (ϕ) can be calculated anywhere along the crack front,

where ϕ is the elliptical angle of a point on the crack front being evaluated. The following expression is used in calculating K_I (ϕ).

$$K_I = \left[\frac{\pi a}{Q}\right]^{0.5} \sum_{j=0}^{4} G_j\left(a/c,\, a/t,\, t/R,\, \phi\right) A_j\, a^j$$

The magnification factors G_0, G_1, G_2, G_3 and G_4 can be found in [6]. The parameter "a" is the crack depth, "c" is the half crack length, "t" is the wall thickness, "R" is the mean radius, "ϕ" is the parametric angle of the elliptical crack, and "Q" is the shape factor.

2.2.5 Fatigue Crack Growth Analysis

The applied loads used in the fatigue crack growth analysis include pressure, thermal transients and residual stresses. The normal and upset thermal transients considered in the fatigue crack growth analysis are shown in Table 2-2. The transient cycles are distributed evenly over the entire plant design life. The crack tip stress intensity factor range, ΔK, which controls fatigue crack growth, depends on the geometry of the crack, its surrounding structure and the range of applied stresses in the region of the crack. Once ΔK is calculated, the fatigue crack growth due to a particular stress cycle can be determined using a crack growth rate reference curve applicable to the head penetration nozzle material.

The fatigue crack growth rate (CGR) reference curve used in the fatigue crack growth analysis for the Alloy 600 material in air environment is based on that in NUREG/CR-6721 [7] and is shown below.

$$\frac{da}{dN} = C S_R \Delta K^{4.1}$$

$$C = 4.835\times10^{-14} + 1.622\times10^{-16}T - 1.490\times10^{-18}T^2 + 4.355\times10^{-21}T^3$$

$$S_R = \left[1 - 0.82R\right]^{-2.2}$$

where:

T = Temperature of the Transient (°C)

ΔK = Stress Intensity Factor Range (MPa$\sqrt{m}$)

R = Stress Ratio (K_{min}/K_{max})

$\frac{da}{dN}$ = Fatigue crack growth rate (meters/cycle)

Once the incremental crack growth corresponding to a specific transient for a given time period is calculated, it is added to the previous crack size, and the analysis continues to the next time period and/or thermal transient assuming the flaw shape remains constant. The procedure is repeated in this manner until all the significant design thermal transients and cycles known to occur in a given period of operation have been analyzed. For conservatism, R=1 is used in the fatigue crack growth analysis.

2.3 Flaw Evaluation Results

The maximum allowable end-of-evaluation period axial and circumferential flaw depths for the V. C. Summer Unit 1 penetration nozzles of interest are provided for various flaw aspect ratios (flaw depth/flaw length) in Table 2-3. The maximum allowable initial axial and circumferential flaw sizes accounting for fatigue crack growth of 40 years after the repair are shown in Figures 2-2 and 2-3 respectively. The maximum allowable initial flaw sizes are obtained by subtracting the fatigue crack growth for 40 years of service life after the repair from the maximum allowable end-of-evaluation period flaw sizes. Figure 2-4 shows the fatigue crack growth for hypothetical axial and circumferential flaws with initial flaw depth and aspect ratios (flaw depth/flaw length) that bound those for the left-behind flaws in repaired penetration nozzle number 19, 31, 37 and 52. The fatigue crack growth curves shown in Figure 2-4 would bound the fatigue crack growth curves for each of the indications in the repaired penetration nozzles of interest. The fatigue crack growth results shown in Figure 2-4 shows that it would take more than 40 years to reach the maximum allowable end-of-evaluation period flaws sizes shown in Table 2-3. This is consistent with the results shown in Figures 2-2 and 2-3 where the left-behind flaw sizes in the repaired penetration nozzles of interest are below the maximum allowable initial flaw size curves.

As shown in Figures 2-2 and 2-3, the respective maximum allowable initial axial and circumferential flaw sizes are larger than the left-behind flaws in the repaired penetration nozzle number 19, 31, 37 and 52. Therefore, all the repaired flaws are acceptable for continued operation for at least 40 years after the repair. It should be noted in Figures 2-2 and 2-3, the aspect ratios (flaw depth/flaw length) for indications in the penetration nozzles are set to a maximum of 0.5 in accordance with the ASME Section XI Code.

Table 2-3
Maximum Allowable End-of-Evaluation Period Flaw Sizes
(Percentage of Nominal Wall Thickness)

Aspect Ratio (Depth/Length)	Circumferential Flaw	Axial Flaw
0.20	57%	75%
0.33	73%	75%
0.50	75%	75%

3.0 Conclusions

The unacceptable outside surface circumferential flaws are isolated from the primary water environment using the Westinghouse embedded flaw repair process. Primary water stress corrosion is no longer a credible degradation mechanism and fatigue is the only credible crack growth mechanism. The left behind flaws in the repaired head penetration nozzle number 19, 31, 37 and 52 have been shown to be acceptable for continued operation for at least 40 years after the repair. These upper head penetration nozzles will be inspected every refueling outage following the repair. It is therefore technically justified to use the embedded flaw repair process as the repair technique for the reactor vessel head penetration nozzles with the unacceptable outside surface flaws since the criteria for application of such a process as stated in Appendix C of WCAP-15987-P is met.

4.0 References

1. Westinghouse WCAP-15987-P, Revision 2-P-A, "Technical Basis for the Embedded Flaw Process for Repair of Reactor Vessel Head Penetrations," December 2003. (Westinghouse Proprietary Class 2)

2. ASME Section XI Code:

   a. ASME Boiler & Pressure Vessel Code, 1998 Edition through 2000 Addenda, Section XI, Rules for Inservice Inspection of Nuclear Power Plant Components.

   b. ASME Boiler & Pressure Vessel Code, 2007 Edition with 2008 Addenda, Section XI, Rules for Inservice Inspection of Nuclear Power Plant Components.

3. Chicago Bridge & Iron Company Drawing No. 40, Contract No. 71-2631, "157" PWR Control Rod Drive Mechanism Housings Details," Revision 6.

4. Dominion Engineering, Inc. Report C-8849-00-01 Rev. 0, "V.C. Summer RPV Head CRDM Nozzle Welding Residual Stress plus Transient Analysis". (Dominion Engineering Inc. Proprietary Document)

5. Design Specification DS-MRCDA-09-10, Revision 0, Equipment: Reactor Vessel – Virgil C. Summer Nuclear Station Addendum to Equipment Specification 679105 Rev. 2. (Westinghouse Proprietary Class 2)

6. American Petroleum Institute, API 579-1/ASME FFS-1 (API 579 Second Edition), "Fitness-For-Service," June 2007.

7. NUREG/CR-6721, ANL-01/07, "Effects of Alloy Chemistry, Cold Work, and Water Chemistry on Corrosion Fatigue and Stress Corrosion Cracking of Nickel Alloys and Welds," April 2001.

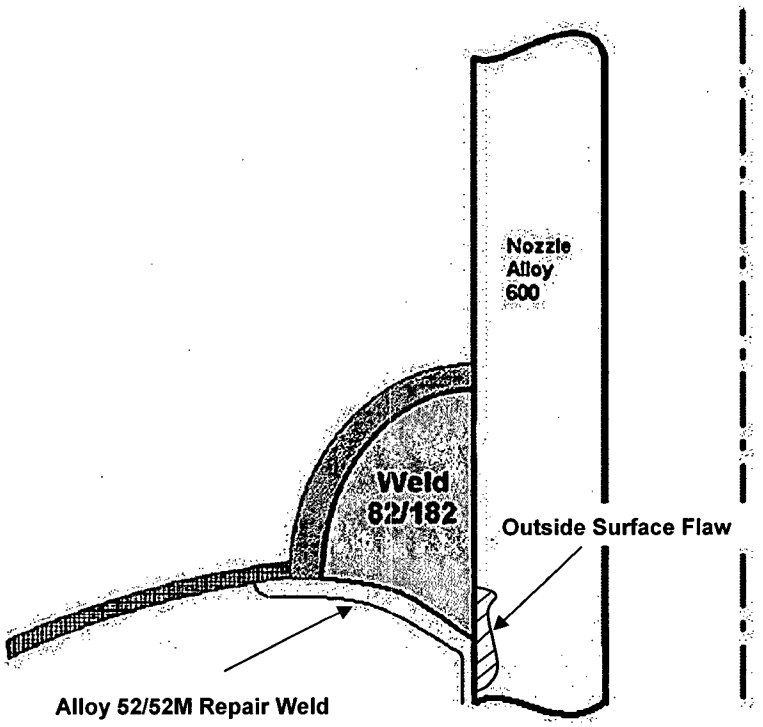

Figure 2-1 A Schematic of the Repair Configuration for the Outside Surface Flaw

Note: The outside surface flaw shown in the figure is for repair configuration illustration purposes and does not intend to represent the actual outside surface flaws detected at V. C. Summer Unit 1

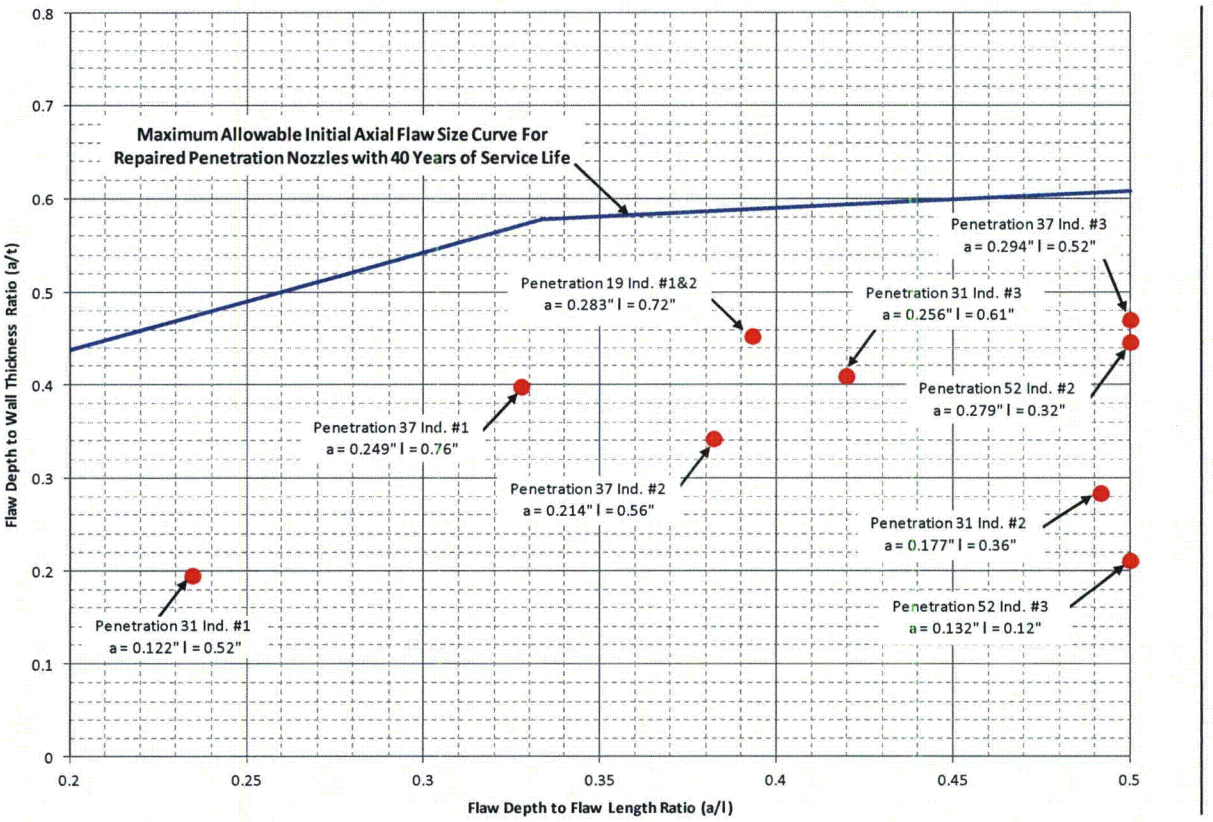

Figure 2-2 Maximum Allowable Initial Axial Flaw Sizes for Repaired Penetration Nozzles

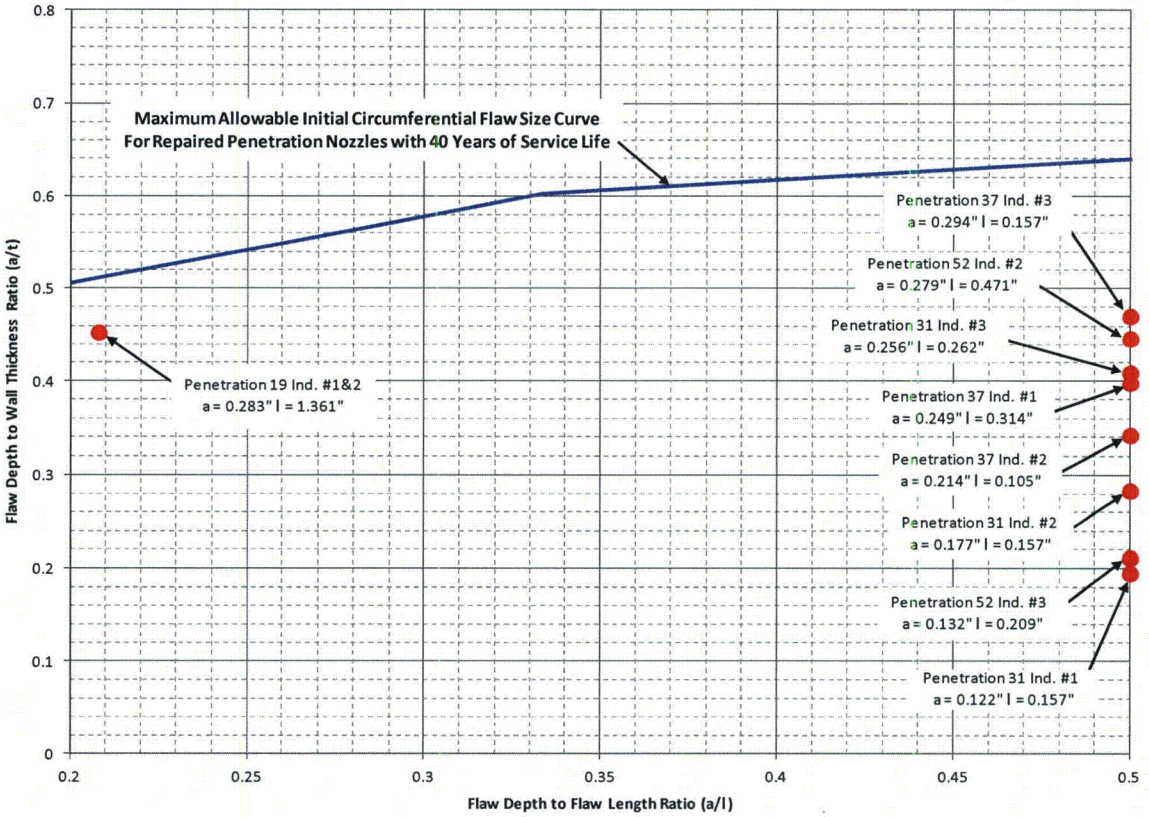

Figure 2-3 Maximum Allowable Initial Circumferential Flaw Sizes for Repaired Penetration Nozzles

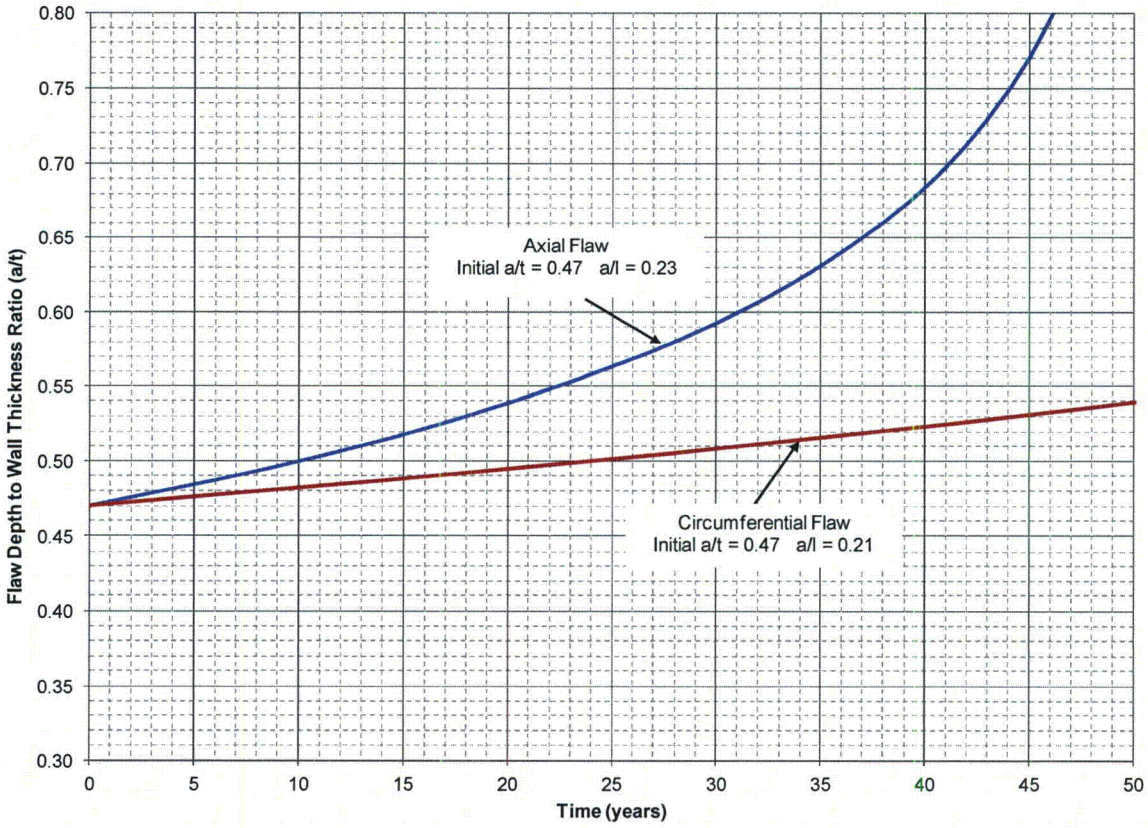

Figure 2-4 Fatigue Crack Growth For Hypothetical Bounding Axial and Circumferential Flaws